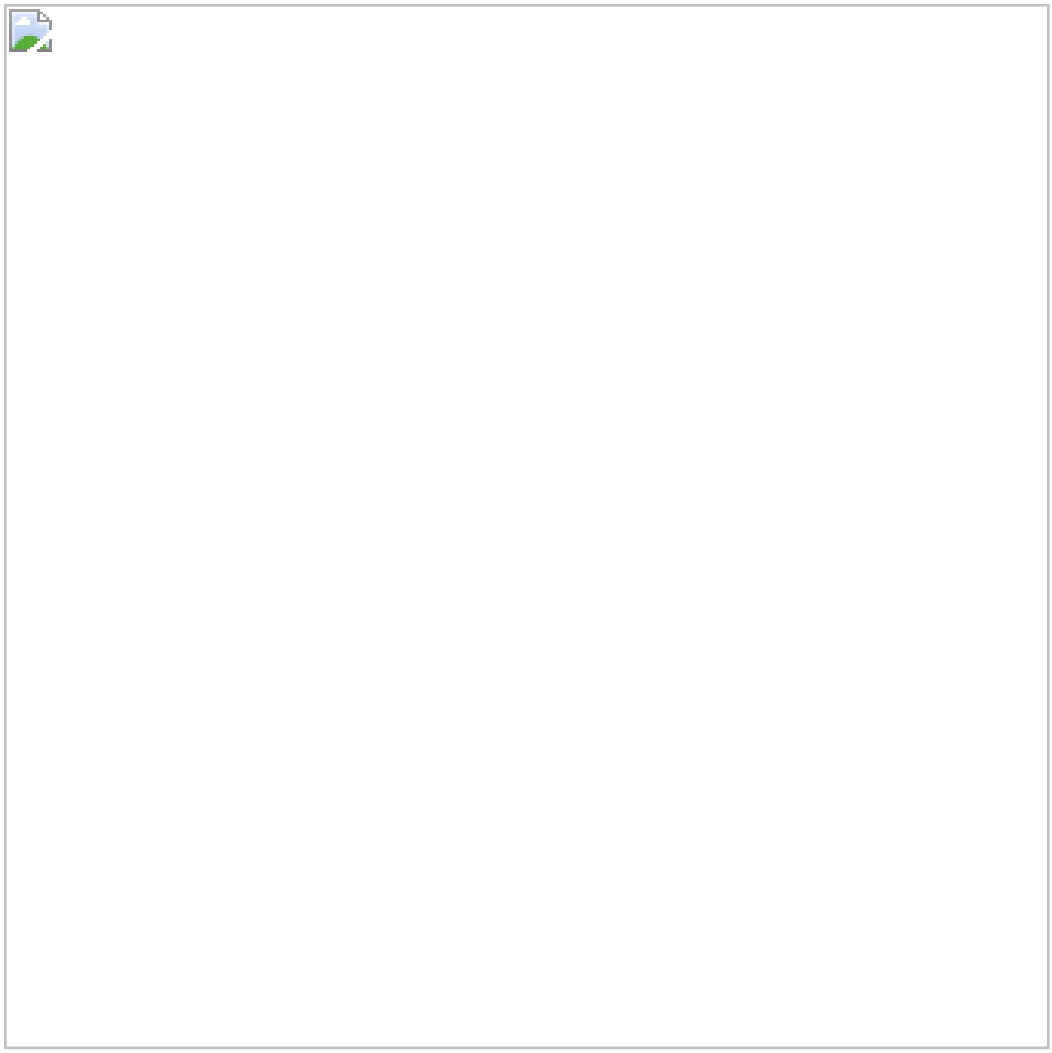

Adsorptive Removal of Phosphate From Wastewater Using Ethiopian Rift Pumice: Batch Experiment

Authors: Fetene, Yohannis, and Addis, Taffere

Source: Air, Soil and Water Research, 13(1)

Published By: SAGE Publishing

URL: https://doi.org/10.1177/1178622120969658

Adsorptive Removal of Phosphate From Wastewater Using Ethiopian Rift Pumice: Batch Experiment

Air, Soil and Water Research
Volume 13: 1–12

DOI: 10.1177/1178622120969658

Yohannis Fetene[1] and Taffere Addis[2]

[1]Ethiopian Environment and Forest Research Institute, Jimma Research Center, Jimma, Ethiopia.
[2]Ethiopian Institute of Water Resources, Addis Ababa University, Addis Ababa, Ethiopia.

ABSTRACT: Phosphorous from municipal and industrial wastewater is the main cause of eutrophication of rivers and lakes, because effluent quality from conventional secondary wastewater treatment plants does not meet the discharge standard that demands further treatment. Therefore, we investigated pumice as a potential low-cost adsorbent for the tertiary treatment of phosphate from municipal wastewater. The phosphate adsorption process reached equilibrium after 60 minutes contact time and achieved a removal efficiency of 94.4% ± 0.7% for an adsorbent dose of 10 g/L in 3 mg/L phosphate solution. The highest phosphate removal was recorded at pH 7. The experimental data best fitted with the Redlich-Peterson isotherm and the pseudo-second-order kinetic models. The coexisting anions decreased phosphate adsorption in the order of mixture $>SO_4^{2-}>HCO_3^->NO_3^->Cl^->CO_3^-$. Pumice removed 95% ± 0.2% of phosphate from effluents of the secondary treatment unit of a municipal wastewater treatment plant. Furthermore, effective regeneration of saturated pumice was possible with a 0.2 M NaOH solution. Therefore, pumice could be a technically workable low-cost reusable adsorbent for phosphate removal from wastewater as a tertiary treatment to curb eutrophication of surface waters. However, further column adsorption study is recommended for a continuous flow system to optimize process design variables and scale up for field applications.

KEYWORDS: Adsorption, eutrophication control, phosphorous, wastewater treatment

RECEIVED: June 22, 2020. **ACCEPTED:** October 7, 2020.

TYPE: Original Research

FUNDING: The author(s) disclosed receipt of the following financial support for the research, authorship, and/or publication of this article: This research was supported by Jimma University, Ethiopia.

DECLARATION OF CONFLICTING INTERESTS: The author(s) declared no potential conflicts of interest with respect to the research, authorship, and/or publication of this article.

CORRESPONDING AUTHOR: Taffere Addis, Ethiopian Institute of Water Resources, Addis Ababa University, P.O. Box 1176, Addis Ababa, Ethiopia.
Email: taffere.addis@aau.edu.et

Introduction

Water is an essential resource for human survival, economic development, and the proper functioning of ecosystems. However, due to exponential population growth, rapid industrialization and urbanization, and expansion of agriculture, the water demand has increased tremendously and resulted in the generation of large volumes of wastewater, which contain a higher concentration of various pollutants including phosphate that adversely impacts the environment and ecosystems.[1-3] Excessive phosphate enrichment is the most common cause of eutrophication of freshwater lakes, reservoirs, streams, and headwaters of estuarine systems.[4] The adverse environmental impacts of eutrophication are the reduction of biodiversity, harmful algal blooms, increasing the turbidity of water bodies, and decreasing the storage volume of lakes and reservoirs.[5]

Phosphate removal from wastewater is challenging and calls for innovation in treatment technology development. Phosphate removal techniques fall into physical, chemical, and biological treatment methods.[6,7] The phosphate removal efficiency of physical conventional wastewater treatment methods is very low (5%-10%), and those efficient ones such as electrodialysis and reverse osmosis are too expensive. As a result, chemical precipitation is the most widely used method to remove phosphate from wastewater. However, chemical treatment methods are not sustainable due to high operational cost for chemicals and due to an increase in chemical sludge volume up to 40% that are hard to dispose of, and neutralization of the effluent has various drawbacks.[8,9] Moreover, because most phosphorus compounds in wastewater are water-soluble, precipitation using chemical treatment removes only a small fraction.[10]

In conventional biological wastewater treatment, phosphate removal efficiency usually does not exceed 30%. The effluent quality remains high above discharge standard limits[10,11] that demands further treatment by integrating with other removal techniques. In general, conventional wastewater treatment plant effluent consists of about 3 to 4 mg/L of total phosphorous, of which phosphate comprises 70% to 90%.[12] Among biological treatment methods, enhanced biological phosphorus removal is becoming a standard method.[13-15] However, the technology faces unpredictable failures due to abortive or reduced activity of polyphosphate-accumulating organisms, for example, free nitrous acid generation inhibits biological process.[16,17] Therefore, it has become necessary to develop innovative and low-cost remediation technologies to curb pollution and improve surface water quality.

Different adsorbents such as hybrid impregnated polymeric sorbent containing hydrated ferric oxide,[6] industrial acidified laterite by-product,[18] clay soil,[19] slag and fly ash,[7] activated red mud,[20] steel slags,[21] silicate hybrid materials,[22] ferric oxyhydroxide sulfate,[23] a mixture of sand and dolomite,[24] alginate/goethite hydrogel composite,[25] and $ZnCl_2$ activated coir pith carbon[26] have been investigated for the removal of phosphate from aqueous solution. The chosen adsorbent should be readily available, effective to remove the contaminant, and cheap. Nevertheless, there is no reliable and easily applicable adsorbent for practical application. And the wastewater management sector requires more effective and cheaper adsorbents. As

a result, looking for locally available materials that could be applicable in developing countries, including Ethiopia, is urgent.

Pumice is among the most promising volcanic rocks studied as low-cost adsorbents mainly for heavy metals.[27-31] It has a more comprehensive global distribution in areas with young volcanic fields, including the East Africa countries such as Ethiopia, Eritrea, Kenya, and Tanzania.[32] The Ethiopia Rift, which covers around 30% of the area of the country, is rich in pumice.[33] Few studies on adsorption of phosphate onto pumice reported the material as a promising adsorbent for phosphate removal from wastewater.[34-37] However, the experiments were on synthetic solutions simulated for raw wastewater and landfill leachate. As a result, the initial phosphate concentrations and pumice doses were larger for practical application in tertiary wastewater treatment. Furthermore, the studies did not assess the effect of particle size and major coexisting ions such as CO_3, HCO^{3-}, and NO^{3-}.

Therefore, this batch adsorption study was conducted using synthetic solutions as well as effluents from a secondary treatment unit of a municipal wastewater treatment plant. The study aimed at determining the sorption capacity of phosphate onto pumice; identifying optimum design parameters, such as contact time (5-120 minutes), pH (3-12), adsorbent dose (2-50 g/L), particle size (<0.075-4.75 mm), initial phosphate concentration (0.5-20 mg/L), competing anions (10-100 mg/L), and agitation speed (100-250 r/min); and evaluating the regeneration and reusability potential of pumice for practical application.

This study demonstrated the potential of pumice for phosphate removal from effluents of the secondary treatment unit of a wastewater treatment plant to control eutrophication of surface waters.

Materials and Methods

Adsorbent preparation and characterization

The pumice for this study was collected from the Nazareth area (8.47933° N, 39.24352° E), east of Addis Ababa, in the main Ethiopian Rift. The collected pumice granules were washed with distilled water and dried in an oven at 105°C for 12 hours to remove moisture.[27] After drying, the samples were manually ground using a mortar and pestle and sieved into four sieve size fractions: silt (<0.075 mm), fine (0.075-0.425 mm), medium (0.425-2.0 mm), and coarse (2.0-4.75 mm) in diameter using the American Society for Testing and Materials (ASTM D 422) soil textural classification system.[38] The sieved pumice samples were kept in an airtight plastic container at room temperature until used for the experiment.

We determined the point of zero charge of pumice using 0.01 M NaCl solution as an electrolyte and titrating with 0.1 M solutions of NaOH or HCl.[39] The pH of the electrolyte solution was adjusted to the desired values ranging from 3 to 12 in beakers holding a 50 mL solution. Then a 0.5 g of pumice was added into each beaker and shaken for 48 hours to complete the reaction. Finally, the adsorbent was filtered and measured the final pH of each beaker. The point of zero charge of the pumice was figured out by plotting the initial pH versus the pH after 48 hours of agitation. For pH determination, 0.2 g of the dry and grinded pumice was mixed with 25 mL of distilled water and boiled for 30 minutes in stoppered glass bottle.[40] The pH of the adsorbent was measured using a Model HI-98194 digital multiparameter probe, letting 5 minutes for the pH probe to equilibrate. The chemical composition, specific surface area, porosity, particle density, and cation exchange capacity of samples collected from the same area were reported by a previous study.[30] We used pumice samples collected from the same source. The samples were stored in the laboratory at Jimma University.

Preparation of synthetic phosphate solutions

All chemicals used were of analytical grade reagents purchased from the Afro-German Chemicals Est. P.L.C. Phosphate stock solution of 50 mg/L was prepared by dissolving 0.2195 g of anhydrous potassium dihydrogen phosphate (KH_2PO_4) salt in 1 L of distilled water.[41] All working solutions of the desired concentrations were prepared by diluting the stock solution. Potassium salts of chloride, nitrate, sulfate, and the sodium salt of bicarbonate and carbonate anions were used to investigate the effect of competing anions on phosphate adsorption. The pH of the solutions was adjusted by adding 0.1 M NaOH and 0.1 M HCl.

Wastewater effluent sample collection and analysis

The wastewater effluent used in this study was collected from the outlet of a waste stabilization pond located at 7.7° N and 36.8° E in Jimma Town, southwest Ethiopia, in February 2019, dry season in the Ethiopian context. We used composite effluent samples collected four times per day from 8:00 a.m. to 5:00 p.m. at 3 hours interval. The effluent samples were collected using polyethylene bottles washed with distilled water, soaked in 10% HCl overnight, and then rinsed again with distilled water. After sampling, the bottles were stoppered and immediately transported to the Laboratory of Department of Chemistry, Jimma University (Ethiopia). A cold storage at 4°C was maintained from sampling until analysis.

The physicochemical characteristics of both untreated and treated samples were analyzed following standard methods for the examination of water and wastewater.[42] Temperature, pH, and electrical conductivity (EC) were measured using Model HI-98194 multiparameter probe. Titration with sulfuric acid was used for the determination of carbonate and bicarbonate. Chloride and nitrate were measured using the argentometric method and phenoldisulfonic acid method, respectively. Moreover, we used a gravimetric method with ignition of the residue for sulfate, ascorbic acid method for phosphate, open

reflux method for chemical oxygen demand (COD), and modified Winkler's (Azide modification) method for 5-day biological oxygen demand (BOD) determinations.

Adsorption experiment

Batch adsorption experiments were conducted to study the removal process and efficiency of phosphate adsorption on pumice under various experimental conditions. In all experiments, a known concentration of phosphate and the chosen weight of pumice were mixed in 100 mL of solution in a 250-mL acid-washed Erlenmeyer flask. The adsorbent was equilibrated by shaking with 0.01 M $CaCl_2.2H_2O$ for 12 hours before the actual experiment to maintain a constant ionic strength and minimize cation exchange.[30,43] The pH of phosphate solution and pumice mixture was set to 7.0 using 0.1 M HCl and NaOH. Then, the flask with the solution was shaken on a horizontal shaker (SM 30C, Edmund Buhler) at 200 r/min for 60 minutes (equilibrium time) to homogenize and speed up the reaction. Finally, 50 mL of the prepared solutions were centrifuged (Centrifuge 5804, Eppendorf AG, Hamburg, Germany) at 3000 r/min for 15 minutes and the supernatant liquid analyzed for phosphate concentration using a spectrophotometer (Spectrophotometer, V-630 JASCO, Tokyo, Japan) at wavelength of 880 nm.[44]

The adsorption capacity of the adsorbent at any time t and removal efficiency in percent were determined using Equations (1) and (2), respectively[45]

$$q_t = \left(C_o - C_t\right)\frac{V}{M} \tag{1}$$

$$A(\%) = \frac{\left(C_o - C_t\right)}{C_o} \times 100 \tag{2}$$

where q_t is the amount of phosphate adsorbed per unit mass of the adsorbent (mg/g), C_o is the initial concentration of phosphate in the aqueous phase (mg/L), C_t is the concentration of phosphate as phosphorus in the aqueous phase at time t (minutes) in mg/L, M is the dry mass of the adsorbent (g), V is the initial volume of the aqueous phase in contact with the adsorbents during the adsorption test in liter (L), and A (%) is the adsorbed phosphate in percent at time t.[46]

The distribution coefficient (K_D) is the ratio of the concentrations of adsorbate on the adsorbent and in solution at equilibrium conditions. This value indicates the capability of the adsorbent to retain a solute and the extent of its movement in a solution phase.[47] The K_D values of phosphate adsorption onto pumice were calculated using Equation (3) as follows

$$K_D = \frac{q_t}{C_t} \tag{3}$$

where q_t is the concentration of phosphate in the solid particles (mg/g) and C_t is the concentration of phosphate in water (mg/L).

To verify the repeatability of the experimental data, each test was run in duplicate, and the reported data are mean ± standard deviation values. Furthermore, control (only the test solution without adsorbent) and blank (only the adsorbent without the test substance) tests were conducted for each set of experiments. The standard deviations calculated using Microsoft Office Excel 2016 software were less than 2.5%.

Adsorption kinetics and rate-limiting steps

Understanding the adsorption kinetics of pollutants onto adsorbent materials is essential for sizing the adsorption system structure for pollutant removal. Adsorption kinetics was determined by batch experiments involving monitoring of phosphate concentrations over time until equilibrium is reached.[44,48] Pseudo-first-order and pseudo-second-order kinetic models were used to analyze the fitting degrees of the models of phosphate adsorption onto pumice.[29,49] The pseudo-first-order kinetic model is presented using Equation (4)

$$\log\left(q_e - q_t\right) = \log q_e - \frac{K_f t}{2.303} \tag{4}$$

where K_f is the pseudo-first-order rate constant of adsorption (1/min), and q_t and q_e (both in mg/g adsorbent) are the amount of phosphate adsorbed at any time t and at equilibrium, respectively. Straight-line plots of $\log(q_e - q_t)$ versus t were used to calculate rate constants and the determination coefficient (R^2).

The pseudo-second-order kinetic model was evaluated by plotting Equation (5)

$$\frac{t}{q_t} = \frac{1}{K_s q_e^2} + \frac{t}{q_e} \tag{5}$$

where K_s is the pseudo-second-order adsorption rate constant (mg/min). If the pseudo-second-order kinetics is applicable, the plot of t/q_t versus t shows a linear relationship.

The intraparticle diffusion model describes the relationship between potential rate-controlling steps q_t and the square root of time ($t^{0.5}$) as shown in Equation (6)[50]

$$q_t = K_p t^{0.5} + C \tag{6}$$

where q_t is the amount of phosphate adsorbed (mg/g) at a given time t (minutes), k_p [mg/(g.min$^{0.5}$)] is the intraparticle diffusion rate constant, and C (mg/g) is the intercept of the intraparticle diffusion model. If intraparticle diffusion is rate-limiting, q_t versus $t^{0.5}$ will be a straight line and passes through the origin. Otherwise, both surface adsorption and intraparticle diffusion contribute to the reaction rate.

Adsorption isotherms

Adsorption isotherm models are used to assess the relationship between the amount of adsorbate adsorbed per unit mass of the adsorbent and the concentration of adsorbate in the aqueous phase at equilibrium.[46] Langmuir, Freundlich, and Redlich-Peterson models are among the most widely used isotherm models for describing the data of adsorption experiments.[51] These models can be used to determine the design parameters and optimize the operating conditions of the adsorption system. Furthermore, the models help to predict the removal efficiency of the solute and estimate the amount of adsorbent needed to remove ions from aqueous solution.[52] In this work, these three isotherm models were used to investigate the adsorption mechanisms phosphate onto pumice.

The Langmuir isotherm which is valid for monolayer sorption onto the adsorbent surface is given by Equation (7)[53]

$$q_e = \frac{bQ_oC_e}{1+bC_e} \tag{7}$$

where q_e (mg/g) is the amount of phosphate adsorbed per unit mass of adsorbent (pumice), C_e (mg/L) is the phosphate concentration in the liquid phase at equilibrium, Q_o (mg/g) is the Langmuir constant that represents the monolayer adsorption capacity, and b (L/mg) relates to the heat of adsorption. The Langmuir isotherm can be described in terms of the dimensionless constant called a separation factor (R_L) to illustrate the extent to which the adsorption reaction proceeded and evaluate the feasibility of the adsorption process (Equation (8))

$$R_L = \frac{1}{1+bC_o} \tag{8}$$

The shapes of the isotherms are expressed by R_L and values are interpreted as favorable adsorption if $0 < R_L < 1$, unfavorable adsorption if $R_L > 1$, linear adsorption if $R_L = 1$, and irreversible adsorption if $R_L = 0$.

The Freundlich isotherm model, which assumes a multisite adsorption for heterogeneous surfaces, is expressed in Equation (9)

$$q_e = K_F C_e^{1/n} \tag{9}$$

where K_F (L/mg) is related to the total adsorption capacity and 1/n is a dimensionless number related to the intensity of adsorption that indicates the relative distribution of the energy and the heterogeneity of the adsorbate sites.

The Redlich-Peterson isotherm model is an empirical isotherm incorporating three parameters that combine the features of Langmuir and Freundlich isotherms.[46,51] According to this model, the mechanism of adsorption is a blend of the two models and does not follow ideal monolayer adsorption. The Redlich-Peterson model is presented as

$$q_e = \frac{K_R C_e}{1+a_R C_e^{n_R}} \tag{10}$$

where K_R (L/g) and a_R (L/mg) are parameters of the Redlich-Peterson isotherm equation, and n_R is the Redlich-Peterson exponent (dimensionless) that lies between 0 and 1.

Linearization of adsorption isotherms data might change the error structure of experimental data.[51] Therefore, nonlinearized regression analysis that provides a mathematically rigorous method for determining adsorption parameters using the original form of isotherm equations becomes the preferred option to select the best-fit model, because these methods minimize error distribution between the experimental and predicted data. Thus, we used the sum of the square of errors (SSE), hybrid fractional error function (HYBRID), sum of the absolute errors (EABS), average relative error (ARE), Marquardt's percent standard deviation (MPSD), coefficient of determination (R^2), Spearman's correlation coefficient (r_s), the standard deviation of relative errors (SRE), and nonlinear chi-square test (χ^2) to identify the most best-fit isotherm model in describing the adsorption process of phosphate onto pumice. The mathematical statements of these error functions are summarized in Table 1.

Results and Discussion

Effect of contact time

The effect of contact time on phosphate adsorption onto pumice was investigated by adding 10 g/L pumice in 100 mL of an aqueous solution of 3 mg/L phosphate in volumetric flasks. The phosphate removal efficiencies were 49.4% ± 2.2%, 82.5% ± 0.9%, 88.1% ± 2.3%, 94.2% ± 0.9%, and 94.4% ± 0.7% for a contact time of 5, 15, 30, 45, and 60 minutes, respectively (Figure 1). The adsorption rate increased sharply up to 15 minutes and then gradually reached equilibrium after 60 minutes of reaction time. However, previous studies[31,55] on removing heavy metals from water by adsorption using pumice reported a longer equilibrium time (>2 hours), indicating that pumice has a higher affinity and specificity to phosphate than heavy metals.

Effect of pH

Phosphate adsorption onto pumice is dominated by a complexation reaction between surface groups and the adsorbing molecules. Depending on the pH, the pumice surface sites react as an acid or base and result in a pH-dependent surface charge causing electrostatic interactions with the surrounding aqueous phase.[20] Phosphate adsorption onto pumice showed a maximum removal (93.2% ± 1.7%-95.4% ± 1.1%) within pH 3 to 7 and decreased sharply beyond this pH range (Figure 2). A similar result was observed for phosphate adsorption onto Fe-coordinated amino-functionalized three-dimensional

Table 1. List of error functions with mathematical expressions.[46,52,54]

ERROR FUNCTIONS	ABBREVIATIONS	EQUATIONS
Sum of square error	SSE	$\sum\left(q_{e,cal}-q_{e,exp}\right)^2$
Hybrid fractional error function	HYBRID	$\frac{100}{n-p}\sum_{i=1}^{n}\left[\frac{q_{e,exp}-q_{e,cal}}{q_{e,exp}}\right]^2$
Sum of absolute errors	EABS	$\sum\left\|q_{e,cal}-q_{e,exp}\right\|$
Average relative error	ARE	$\frac{100}{n-p}\sum_{i=1}^{n}\left[\frac{q_{e,exp}-q_{e,cal}}{q_{e,exp}}\right]^2$
Marquardt's percent standard deviation	MPSD	$100\sqrt{\frac{1}{n-p}\sum_{i=1}^{n}\left[\frac{q_{e,exp}-q_{e,cal}}{q_{e,exp}}\right]^2}$
Coefficient of determination	R^2	$\frac{\left(q_{e,mexp}-q_{e,cal}\right)^2}{\sum\left(q_{e,mexp}-\overline{q_{e,cal}}\right)^2+\left(q_{e,mexp}-q_{e,cal}\right)^2}$
Spearman's correlation coefficient	r_s	$1-\frac{6\sum_{i}^{n}\left(q_{e,exp}-q_{e,cal}\right)^2}{n(n-1)^2}$
Standard deviation of relative errors	SRE	$\sqrt{\frac{\sum_{i}^{n}\left[\left(q_{e,exp}-q_{e,cal}\right)^2-ARE\right]^2}{n-1}}$
Nonlinear chi-square test	χ^2	$\sum_{i=1}^{n}\frac{\left(q_{e,cal}-q_{e,exp}\right)^2}{q_{e,exp}}$

Remark: $q_{e,exp}$ (mg/g) is equilibrium adsorption capacity of experimental data, $q_{e,cal}$ (mg/g) is equilibrium adsorption capacity calculated from the model, $q_{e,mexp}$ (mg/g) is mean of $q_{e,exp}$ (mg/g), n is the number of data points, and p is the number of parameters for the model.

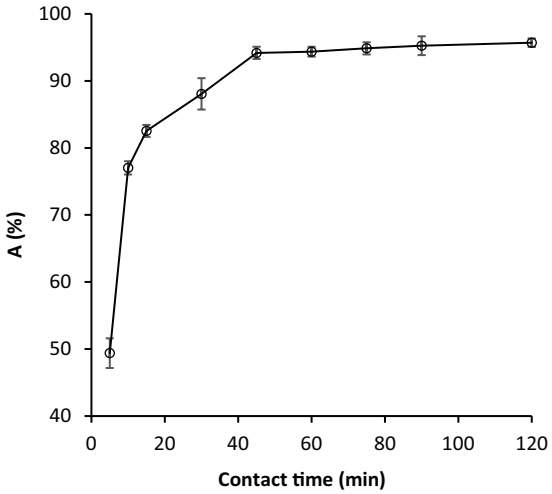

Figure 1. Effect of contact time on phosphate adsorption onto pumice.

(3D) mesoporous silicate hybrid materials[22] and $ZnCl_2$ activated coir pith carbon[26] which is related to phosphate proton dissociation equilibria.[56] At pH values less than the point of zero charges (pH_{ZPC}) of the adsorbent, the net surface charge is positive and eases the adsorption of anions. The pH_{ZPC} of pumice was found to be 9.3. At pH values between 3 and 6, phosphate occurs mainly in the monovalent form of $H_2PO_4^-$, whereas at higher pH values, the divalent anion HPO_4^{2-} dominates ($pK_{a1}=2.23$, $pK_{a2}=7.21$, $pK_{a3}=12.32$).[57] So, it is evident that in the pH range of natural waters, phosphate remains in the anionic state, which is highly favorable for adsorption, because the adsorbent surface remains positively charged owing to its higher pH_{ZPC}. The surface charge of pumice becomes more negative with increasing pH, resulting in a more neutral and then negatively charged group on the surface.[58] The higher pH not only causes the adsorbent surface to carry more

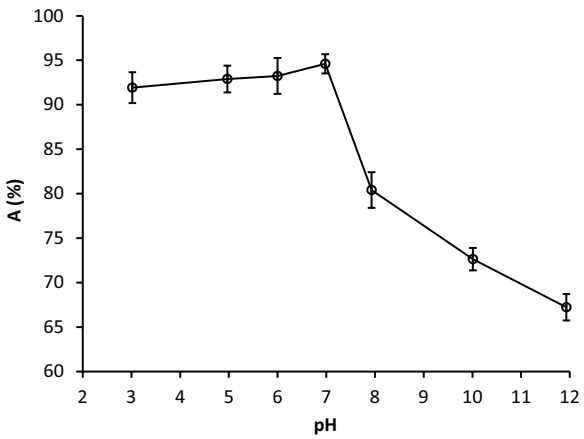

Figure 2. Effect of pH on phosphate adsorption onto pumice.

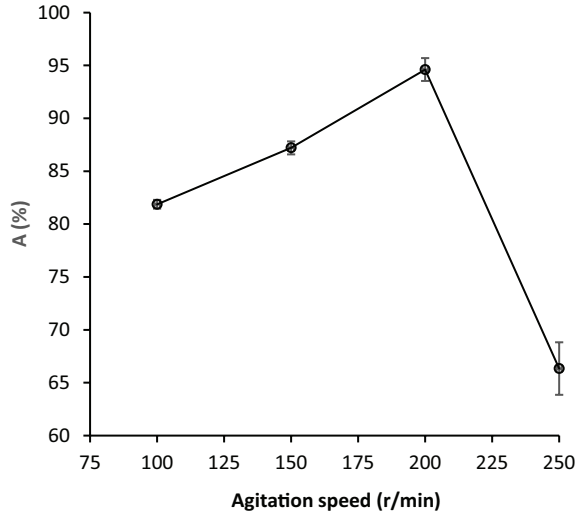

Figure 3. Effect of agitation speed on phosphate adsorption onto pumice.

negative charges but also leads to a high concentration of hydroxide groups. Therefore, there may also be high competition between negatively charged phosphate species and hydroxide groups for positively charged adsorbent surface sites at higher pH values that decrease phosphate adsorptive removal.

Effect of mixing speed

The effect of mixing speed was studied by agitating aqueous solutions of 3 mg/L phosphate and 10 g/L pumice using a horizontal shaker with agitation speed ranging from 100 to 250 r/min for 60 minutes contact time and at a pH of 7. Phosphate adsorption onto pumice increased with increasing agitation speed, reaching a maximum of 94.6% ± 1.1% removal at 200 r/min, and a further increase in agitation speed to 250 r/min, the phosphate removal decreased to 66.3% ± 2.5% (Figure 3). The increase in the percentage of phosphate removal is due to the dispersal of the adsorbent particles in the aqueous solution, which leads to reduced boundary mass transfer resistance that increases the percent removal of

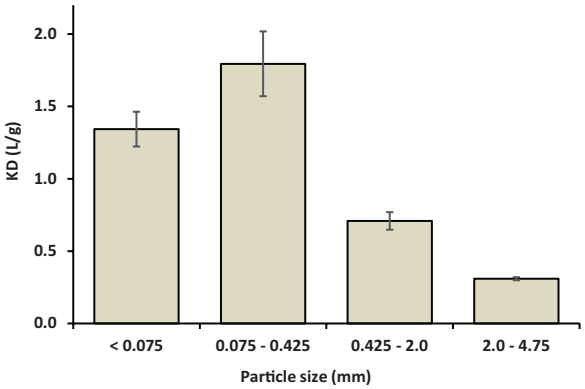

Figure 4. Effect of particle size on phosphate adsorption onto pumice.

phosphate.[20] However, a further increase in mixing speed could promote desorption because the adsorbent pore size might expand as well as repulsive force to phosphate at the interface (more like charges approach the interface and repel) get higher and increase the release of adsorbed phosphate from pumice.

Effect of particle size of the adsorbent on phosphate removal

We investigated the effect of particle size of the pumice on phosphate adsorption at an initial phosphate concentration of 3 mg/L, the dose of adsorbent = 10 g of pumice/L, agitation speed = 200 r/min, contact time = 60 minutes, and pH = 7. The particle size class of 0.075 to 0.425 mm was found to be the most effective, yielding a maximum phosphate removal efficiency of 94.6% ± 1.1%. The results presented in Figure 4 revealed that the coefficient of distribution, K_D, increased with a decrease in particle size of pumice from 4.75 to 0.075 mm. However, pumice with particle sizes smaller than 0.075 mm did not show enhanced removal, which might be related to losing its porosity, and thus of diffusion-controlled sorption of phosphate.[28]

Effect of pumice dose on adsorption

The optimum dose of pumice as an adsorbent was studied in a dose ranging from 2 to 50 g/L keeping other variables constant (initial phosphate concentration = 3 mg/L, pH = 7, pumice particle size = 0.075-0.425 mm, t = 60 minutes, and agitation speed = 200 r/min). With an increase in adsorbent dose from 2 to 10 g/L, the removal efficiency of phosphate at equilibrium increased sharply from 72.6% ± 1.3% to 94.6% ± 0.9 % (Figure 5). When the pumice dose increased further from 10 to 50 g/L with an interval of 5, or 10, and later 20, the increase in the percentage of phosphate removal was negligible (3.5%). Therefore, 10 g/L was the chosen optimum dose for further adsorption experiments.

The distribution coefficient, K_D, reflects the scavenging and adsorbing ability of the adsorbent for contaminants, which

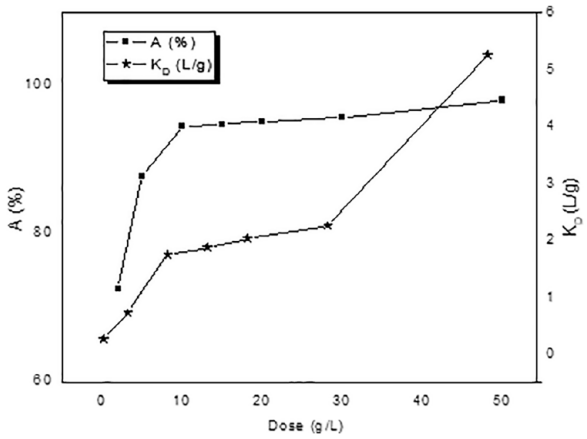

Figure 5. Effect of pumice dose on phosphate adsorptive removal.

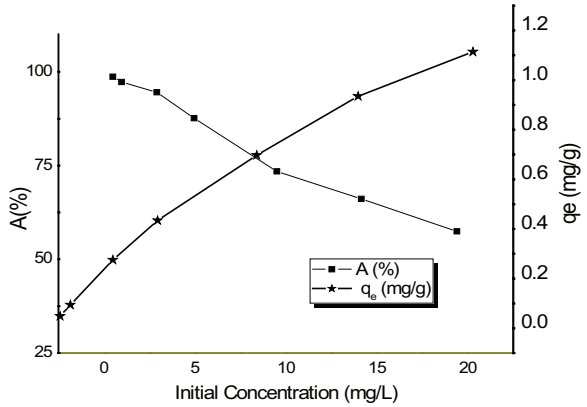

Figure 6. The effect of initial concentration of phosphate on its adsorptive removal by pumice.

estimates the extent of contaminant retardation from adsorbent to water and is known to be dependent on the pH of the surface of the adsorbent.[59] The K_D values for phosphate adsorption onto pumice, which determined at pH 7, increased with an increase in adsorbent dose, indicating the heterogeneity of the surface of pumice.[60] The pumice doses incremental intervals were 5, 10, and 20 g/L from lower to higher doses. The sharp increase in K_D when the doses increased from 30 to 50 g/L might be due to the presence of many adsorption sites that scavenge and take out phosphate more irreversibly that increases K_D value sharply.

Effect of initial phosphate concentration

The effect of the initial phosphate concentration ranging from 0.5 to 20 mg/L on adsorption efficiency and equilibrium uptake was assessed at pH 7 using 10 g/L of pumice. The uptake of phosphate onto pumice increased with increasing its initial concentration (Figure 6). With an increase in the initial concentration of phosphate from 0.5 to 20 mg/L, the absolute amount of phosphate ions per unit mass of adsorbent increased from 0.0486 to 1.1143 mg of phosphate per gram of pumice. This finding is similar to the results of various researchers that suggest the more concentrated solution had more adsorption capacity per unit mass of the adsorbent because the adsorbate is available in a sufficient amount to get adsorbed.[20,29]

However, the percentage of phosphate removal decreased with an increasing initial concentration of phosphate. When the phosphate concentration increased from 0.5 to 20 mg/L, the removal of phosphate decreased from 98.7% ± 1.6% to 57.4% ± 0.1%. This finding is in agreement with the principle of adsorption that sites with a greater affinity toward adsorbate occupied first, followed by other sites with less affinity until the adsorbent reaches its saturation point.[21]

Effects of coexisting ions

Phosphate in wastewater always coexists with other ions such as nitrate, sulfate, chloride, carbonate, and bicarbonate that could compete for the available active adsorption sites on pumice and thereby reduce phosphate adsorption. Therefore, we studied the effect of each competitive ion on the uptake of phosphate by using 10, 100, and 300 mg/L of HCO^{3-}, CO_3^{2-}, Cl^-, NO^{3-}, SO_4^{2-}, and the mixture by adding 10 g/L pumice in 100 mL of an aqueous solution which had an initial phosphate concentration of 3 mg/L. Phosphate removal decreased with an increase in the concentration of the ions from 10 to 300 mg/L. Among these competing anions, bicarbonate and sulfate revealed a higher interfering effect on the adsorption of phosphate onto pumice. The order of interference for phosphate removal onto pumice was the mixture $> SO_4^{2-} > HCO^{3-} > NO_3^- > Cl^- > CO_3^{2-}$ (Figure 7). A similar trend was reported for Fe-coordinated amino-functionalized 3D mesoporous silicate hybrid materials[22] and rice husk–derived biochar functionalized with Mg/Al-calcined layered double hydroxides[61] based adsorption study for phosphate removal. The decrease in the adsorption capacity could be because of ion exchange mechanisms where SO_4^{2-} and HCO^{3-} possess the highest affinity for the adsorbent material and compete most effectively against phosphate adsorption.

The interference with phosphate removal is minimal in the presence of monovalent and divalent anions, which could be attributable to its superior partial negative charges associated with oxygen atoms when compared with other coexisting anions.

Adsorption kinetics

The kinetics of phosphate adsorption onto pumice was studied using 10 g/L adsorbent dose, 3 mg/L phosphate concentration, and agitated for 60 minutes at the pH of 7. The linear plots of the pseudo-first-order, pseudo-second-order, and intraparticle diffusion sorption kinetics constant values of K_1, K_2, K_p, $q_{e,cal}$ (calculated), and $q_{e,exp}$ (experimental) are shown in Table 2. The plots of t/q_t versus t followed a straight line (Figure 8) with the coefficients of determination, $R^2 > 0.99$. Besides, the values of the modeled equilibrium capacities, $q_{e,calc}$ (0.2402, 0.2910),

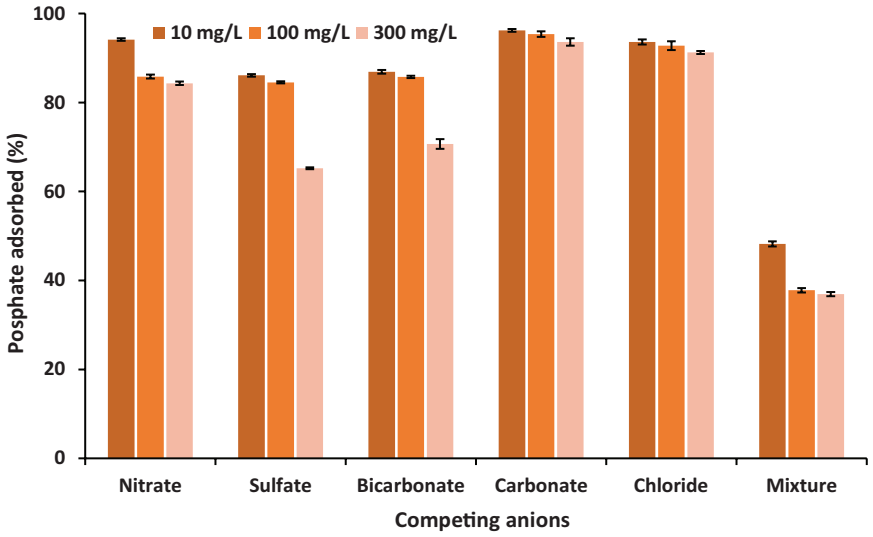

Figure 7. Effect of coexisting anions on the adsorption of phosphate onto pumice.

Table 2. The kinetics parameters for adsorption of phosphate onto pumice.

PSEUDO-FIRST ORDER		PSEUDO-SECOND ORDER		INTRAPARTICLE DIFFUSION	
PARAMETERS	VALUE	PARAMETERS	VALUE	PARAMETERS	VALUE
$q_{e,exp}$ (mg/g)	0.2779	$q_{e,exp}$ (mg/g)	0.2779	K_p [mg/(g.min$^{0.5}$)]	0.0211
$q_{e,calc}$ (mg/g)	0.2402	$q_{e,calc}$ (mg/g)	0.2910	C (mg/g)	0.1045
K_f [g/(mg.min)]	0.1232	K_s [g/(mg.min)]	1.0464	R^2	0.6708
R^2	0.8962	V_o [mg/(g.min)]	0.0886		
		R^2	0.9996		

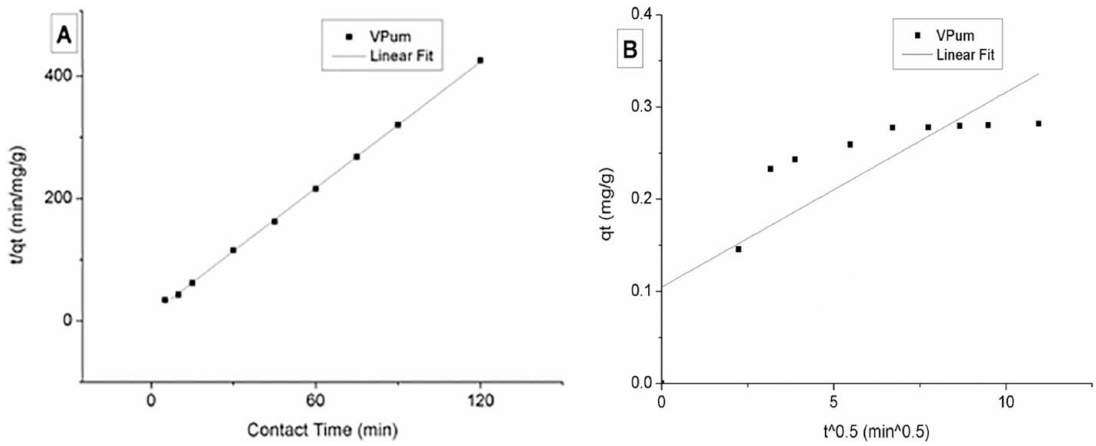

Figure 8. Plot of pseudo-second-order model (A) and intraparticle diffusion model (B) for phosphate adsorption onto pumice.

were comparable with the experimental equilibrium capacities, $q_{e,exp}$ (0.2779) (Table 2). Thus, the kinetics of phosphate adsorption on pumice was well described by the pseudo-second-order equation that indicates the rate-limiting step could be surface chemical adsorption involving valence forces through the sharing or exchange of electrons between adsorbent and adsorbate.[62] Similar results were reported for phosphate removal from wastewater using palm fibers (*Phoenix dactylifera* L.)[63] and ferric oxyhydroxide sulfate.[23]

In addition to the surface adsorption, phosphate may also be diffused into the interior part of the adsorbent depending on the size and pore structure of the adsorbent.[63] Therefore, the intraparticle diffusion model proposed by Weber and Morris (Equation (6))[50] was used to determine whether the particles' diffusion is the rate-limiting step for phosphate adsorption onto pumice. The intraparticle diffusion rate constant (K_p) estimated from the slope of the plot of q_t versus the square root of time ($t^{0.5}$) was found to be 0.0211 mg/(g.min$^{0.5}$) (Table 4). If

Table 3. Error functions of isotherm models.

ISOTHERM MODELS	ERROR FUNCTIONS								
	SSE	HYBRID	ARE	EABS	MPSD	R^2	R_S	SRE	χ^2
Langmuir	0.043	46.338	33.10	0.465	54.508	0.971	0.999	0.461	0.168
Freundlich	0.003	20.793	14.85	0.148	27.969	0.997	1.000	0.270	0.028
Redlich-Peterson	0.002	6.627	4.73	0.090	8.521	0.998	1.000	0.083	0.006

Abbreviations: ARE, average relative error; EABS, sum of the absolute errors; HYBRID, hybrid fractional error function; MPSD, Marquardt's percent standard deviation; SSE, sum of the square of errors.

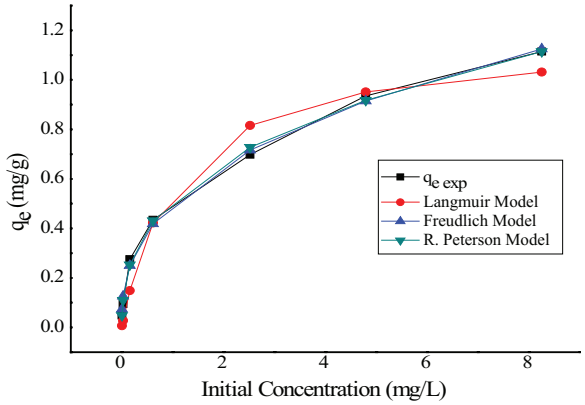

Figure 9. Isotherms of adsorption of phosphate onto pumice.

intraparticle diffusion is a rate-limiting step, the plot should be linear and pass through the origin. In this study, the plot of q_t versus $t^{0.5}$ does not pass through the origin (Figure 8), indicating that phosphate adsorption onto pumice is a complex process with some degree of boundary layer control, and the intraparticle diffusion was not the sole rate-controlling step.[64]

Isotherm models

The best-fit isotherm model for phosphate adsorption onto pumice was selected by evaluating six different error functions. The isotherms of phosphate adsorption at the equilibrium are graphically presented in Figure 9, whereas the values of the equilibrium constants of the models computed using error estimation methods are given in Table 3. The best model is the one which had the highest R^2, and r_s as well as the lowest SSE, HYBRID, EABS, ARED, MSPED, RESID, and χ^2 values. The examination of all these error estimation methods showed that the Redlich-Peterson model best fits the experimental equilibrium data.

Among the linear analysis, the regression coefficient (R^2) was the highest, which makes it more suitable as an error estimation tool to determine the best-fit isotherm model. In the nonlinear analysis, ARED, MSPED, HYBRID, RESID, and SSE were the most appropriate ones, similar to a previous study.[54] These error estimation statistical tools revealed that the Redlich-Peterson model is the best-fitting model. The Redlich-Peterson isotherm model combines the features of the Langmuir and Freundlich isotherm models. Therefore, both monolayer surface reaction and multilayer heterogeneous surface reaction play a significant role in the adsorption of phosphate onto pumice. However, the multilayer heterogeneous surface role seems dominant because it is the second best-fit model next to the Redlich-Peterson isotherm model.[51]

Moreover, the Freundlich constant 1/n can also be a measure of adsorption intensity/surface heterogeneity as well as a measure of deviation from the linearity of adsorption. If 1/n = 1 and the adsorption plot is linear, the adsorption sites are homogeneous in energy, and no interaction occurs between the adsorbed species.[46] The calculated 1/n value for pumice adsorbent was less than unity (0.38) (Table 4) that indicated phosphate removal onto the pumice is favorable and spontaneous, and chemical adsorption is dominant.[64] The larger Langmuir monolayer capacity (Q_o) shows strong interactions between phosphate and pumice (Figure 9). Besides, the R_L values for the experimental data fell between 0 and 1 (Table 4), indicating the favorable adsorption of phosphate onto pumice.[53]

Removal of phosphate from wastewater

As phosphate removal capacity of pumice from synthetic aqueous solution was found to be promising, the adsorption of phosphate onto pumice was further tested for effluents from municipal waste stabilization pond at optimized conditions of adsorbent dose, particle size, contact time, and mixing rate. The phosphate removal efficiency was found to be 95% ± 0.2%, which is greater than the Ethiopian discharge standard for the industrial and municipal wastewater treatment plants.[65] Besides, pumice polished further the concentrations of COD, BOD, nitrate, chloride, and sulfate (Table 5). However, these contaminants could reduce phosphate removal efficiency if the concentrations are higher, which demand adequate pretreatment systems such as grease/oil removal chambers and properly operated septic tank system followed by conventional biological treatment.

Adsorbent regeneration experiment

An adsorbent is economically viable for pollutant removal from aqueous environments if it can be regenerated and reused.[48] The effect of pH on the efficiency of phosphate adsorption onto pumice was very low at pH above 7, suggesting the possibility of

Table 4. Freundlich, Langmuir, and Redlich-Peterson isotherm model constants for phosphate adsorption onto pumice.

FREUNDLICH		LANGMUIR		REDLICH-PETERSON	
PARAMETERS	VALUE	PARAMETERS	VALUE	PARAMETERS	VALUE
K_F (L/g)	0.50	Q_o (mg/g)	1.17	K_R (L/g)	15.81
1/n	0.38	b (L/g)	0.92	a_R (1/mg)	29.52
R^2	0.997	R^2	0.971	n_R	0.64
		R_L	0.271	R^2	0.998

Table 5. Physicochemical characteristics of waste stabilization pond effluent and phosphate removal efficiency of pumice adsorbent.

PARAMETERS	UNTREATED EFFLUENT	TREATED EFFLUENT	EFFICIENCY (%)
Temperature (°C)	24.0 ± 0.7	24.4 ± 0.3	—
pH	5.4 ± 0.1	6.2 ± 0.1	—
EC (μS/cm)	342 ± 5.7	386 ± 6.0	—
COD (mg/L)	480 ± 8.5	292 ± 7.1	39 ± 0.4
BOD (mg/L)	384 ± 9.9	293 ± 7.9	24 ± 0.1
NO^{3-} (mg/L)	271 ± 2.8	175 ± 4.2	36 ± 2.2
Cl^- (mg/L)	55 ± 1.4	36 ± 2.8	35 ± 6.8
SO_4^{2-} (mg/L)	2.7 ± 0.2	1.9 ± 0.1	31 ± 7.1
HCO^{3-} (mg/L)	92 ± 1.4	39 ± 0.7	56 ± 0.1
PO_4^{2-}—P (mg/L)	6.9 ± 0.1	0.14 ± 0.02	95 ± 0.2

Abbreviations: BOD, biological oxygen demand; COD, chemical oxygen demand; EC, electrical conductivity.

desorbing phosphate from the saturated pumice using an alkaline solution. Thus, batch desorption of phosphate was carried out under identical experimental conditions of the batch sorption studies using 100 mL of 0.1 and 0.2 M NaOH solutions. The desorption efficiency in percent is defined as the amount of phosphate desorbed from per gram of spent adsorbent at equilibrium, that is, the ratio of q_e of desorption to q_e of adsorption of adsorbent multiplied with 100.[66,67] The q_e of desorption was calculated as

$$q_e = V\left(\frac{C_f}{M}\right) \quad (11)$$

where M is the weight of spent pumice adsorbent (g), V is the volume of the NaOH solvent (L), and C_f is the equilibrium phosphate concentration in the desorption solution (mg/L).

The percentages of phosphate desorbed at pH > 12 using 0.1 and 0.2 M NaOH solutions for the first cycle desorption experiment were 83% ± 0.8% and 98% ± 1.1%, respectively (Table 6). Two more cycles of adsorption-desorption studies

Table 6. Efficiency of desorption of phosphate from pumice using NaOH solutions.

CYCLE	ADSORPTION (%)	DESORPTION (%)	
		0.1 M NAOH	0.2 M NAOH
1	95 ± 0.2	83 ± 0.8	98 ± 1.1
2	90 ± 0.5	78 ± 0.9	95 ± 0.8
3	77 ± 0.3	71 ± 1.0	93 ± 0.6
4	75 ± 0.7	—	—

were conducted to evaluate the adsorption capacity of the regenerated adsorbent for repeated reuse. In the third cycle, the adsorbent phosphate removal efficiency was 77% ± 0.3%, while that of the fourth cycle was 75% ± 0.7%, which is still high. Therefore, pumice has reusability potential for phosphate removal from wastewater.

Conclusions

This study gives valuable information about the adsorption process of phosphate removal from wastewater by using pumice. Phosphate adsorption onto pumice reached equilibrium after about 60 minutes. The highest phosphate removal has occurred at pH 7, which is suitable for practical applications. The phosphate adsorption removal by pumice reduced in the presence of competing anions in the order of mixture $> SO_4^{2-} > HCO^{3-} > NO_3^- > Cl^- > CO^{3-}$. The experimental data fitted well to the Redlich-Peterson isotherm model and pseudo-second-order kinetic model suggesting the dominance of the chemisorption mechanism for phosphate adsorption onto pumice. Pumice removed 95% ± 0.2% of phosphate from the effluent of the municipal waste stabilization pond that had 6.9 mg/L of phosphate. Besides, saturated pumice effectively regenerated using 0.2 M NaOH solutions that confirm the reusability potential of pumice. Therefore, pumice is an abundant and widely available adsorbent that could be considered as a technically workable and economically viable adsorbent to remove phosphate from effluents of the secondary wastewater treatment plants to control eutrophication of surface waters. However, further column adsorption experiments for a continuous flow system will be needed to optimize process variables and scale up for field applications.

Acknowledgements

The authors are thankful to Jimma University for financial and logistic support. The comments of the two anonymous reviewers and editors helped to enrich the readability of this manuscript.

Author Contributions

YF contributed in designing the study, preparation and characterization of adsorbent, conducting the experiment, collecting and analyzing the data, writing and reviewing. TA contributed in developing the content of the manuscript, statistical analysis and interpretation, and writing and reviewing of the manuscript. All authors read and approved the final manuscript.

ORCID iD

Taffere Addis https://orcid.org/0000-0003-1647-4131

REFERENCES

1. Moss B. Water pollution by agriculture. *Philos Trans R Soc B Biol Sci*. 2008; 363:659-666. doi:10.1098/rstb.2007.2176.
2. Flörke M, Kynast E, Bärlund I, Eisner S, Wimmer F, Alcamo J. Domestic and industrial water uses of the past 60 years as a mirror of socio-economic development: a global simulation study. *Glob Environ Chang*. 2013;23:144-156. doi:10.1016/J.GLOENVCHA.2012.10.018.
3. Zedler JB, Kercher S. Wetland resources: status, trends, ecosystem services, and restorability. *Annu Rev Environ Resour*. 2005;30:39-74. doi:10.1146/annurev.energy.30.050504.144248.
4. Lewis WM, Wurtsbaugh WA, Paerl HW. Rationale for control of anthropogenic nitrogen and phosphorus to reduce eutrophication of inland waters. *Environ Sci Technol*. 2011;45:10300-10305. doi:10.1021/es202401p.
5. Cai T, Park SY, Li Y. Nutrient recovery from wastewater streams by microalgae: status and prospects. *Renew Sustain Energy Rev*. 2013;19:360-369. doi:10.1016/j.rser.2012.11.030.
6. You X, Guaya D, Farran A, Luis J, Valderrama C, Cortina JL. Phosphate removal from aqueous solution using a hybrid impregnated polymeric sorbent containing hydrated ferric oxide (HFO). *J Chem Technol Biotechnol*. 2016;91:693-704. doi:10.1002/jctb.4629.
7. Ragheb SM. Phosphate removal from aqueous solution using slag and fly ash. *HBRC J*. 2013;9:270-275. doi:10.1016/j.hbrcj.2013.08.005.
8. Vasudevan S, Sozhan G, Ravichandran S, Jayaraj J, Lakshmi J, Sheela M. Studies on the removal of phosphate from drinking water by electrocoagulation process. *Ind Eng Chem Res*. 2008;47:2018-2023. doi:10.1021/ie0714652.
9. Wang XJ, Xia SQ, Chen L, Zhao JF, Renault NJ, Chovelon JM. Nutrients removal from municipal wastewater by chemical precipitation in a moving bed biofilm reactor. *Process Biochem*. 2006;41:824-828. doi:10.1016/j.procbio.2005.10.015.
10. Ruzhitskaya O, Gogina E. Methods for removing of phosphates from wastewater. *MATEC Web Conf*. 2017;106:1-7. doi:10.1051/matecconf/201710607006.
11. Bali M, Gueddari M. Removal of phosphorus from secondary effluents using infiltration–percolation process. *Appl Water Sci*. 2019;9:54. doi:10.1007/s13201-019-0945-5.
12. Water Environment Federation. *Biological Nutrient Removal (BNR) Operation in Wastewater Treatment Plants*. Reston, VA: Water Environment Federation and American Society of Civil Engineers; New York, NY: McGraw-Hill; 2006.
13. Oehmen A, Lemos PC, Carvalho G, et al. Advances in enhanced biological phosphorus removal: from micro to macro scale. *Water Res*. 2007;41:2271-2300. doi:10.1016/j.watres.2007.02.030.
14. Izadi P, Izadi P, Eldyasti A. Design, operation and technology configurations for enhanced biological phosphorus removal (EBPR) process: a review. *Rev Environ Sci Biotechnol*. 2020;19:561-593. doi:10.1007/s11157-020-09538-w.
15. Chen Y, Randall AA, McCue T. The efficiency of enhanced biological phosphorus removal from real wastewater affected by different ratios of acetic to propionic acid. *Water Res*. 2004;38:27-36. doi:10.1016/j.watres.2003.08.025.
16. Zhao J, Wang D, Li X, et al. An efficient process for wastewater treatment to mitigate free nitrous acid generation and its inhibition on biological phosphorus removal. *Sci Rep*. 2015;5:8602. doi:10.1038/srep08602.
17. Pan M, Huang X, Wu G, Hu Y, Yang Y, Zhan X. Performance of denitrifying phosphate removal via nitrite from slaughterhouse wastewater treatment at low temperature. *Water*. 2017;9:818. doi:10.3390/w9110818.
18. Glocheux Y, Pasarín MM, Albadarin AB, Mangwandi C, Chazarenc F, Walker GM. Phosphorus adsorption onto an industrial acidified laterite by-product: equilibrium and thermodynamic investigation. *Asia-Pac J Chem Eng*. 2014;9:929-940. doi:10.1002/apj.1843.
19. Mallikarjun SD, Mise SR. A batch study of phosphate adsorption characteristics on clay soil. *Int J Res Eng Technol*. 2013;1:338-342.
20. Baraka AM, El-Tayieb MM, El Shafai M, Mohamed NY. Sorptive removal of phosphate from wastewater using activated red mud. *Aust J Basic Appl Sci*. 2012;6:500-510.
21. Barca C, Gérente C, Meyer D, Chazarenc F, Andrès Y. Phosphate removal from synthetic and real wastewater using steel slags produced in Europe. *Water Res*. 2012;46:2376-2384. doi:10.1016/j.watres.2012.02.012.
22. Zhang J, Shen Z, Mei Z, Li S, Wang W. Removal of phosphate by Fe-coordinated amino-functionalized 3D mesoporous silicates hybrid materials. *J Environ Sci (China)*. 2011;23:199-205.
23. Eskandarpour A, Sassa K, Bando Y, Okido M, Asai S. Magnetic removal of phosphate from wastewater using schwertmannite. *Mater Trans*. 2006;47:1832-1837. doi:10.2320/matertrans.47.1832.
24. Prochaska CA, Zouboulis AI. Removal of phosphates by pilot vertical-flow constructed wetlands using a mixture of sand and dolomite as substrate. *Ecol Eng*. 2006;26:293-303. doi:10.1016/j.ecoleng.2005.10.009.
25. Siwek H, Bartkowiak A, Włodarczyk M. Adsorption of phosphates from aqueous solutions on alginate/goethite hydrogel composite. *Water (Switzerland)*. 2019;11:633. doi:10.3390/w11040633.
26. Namasivayam C, Sangeetha D. Equilibrium and kinetic studies of adsorption of phosphate onto ZnCl2 activated coir pith carbon. *J Colloid Interface Sci*. 2004;280:359-365.
27. Alemayehu E, Lennartz B. Virgin volcanic rocks: kinetics and equilibrium studies for the adsorption of cadmium from water. *J Hazard Mater*. 2009;169:395-401. doi:10.1016/j.jhazmat.2009.03.109.
28. Alemayehu E, Lennartz B. Adsorptive removal of nickel from water using volcanic rocks. *Appl Geochemistry*. 2010;25:1596-1602. doi:10.1016/j.apgeochem.2010.08.009.
29. Khorzughy SH, Eslamkish T, Ardejani FD, Heydartaemeh MR. Cadmium removal from aqueous solutions by pumice and nano-pumice. *Korean J Chem Eng*. 2015;32:88-96.
30. Alemayehu E, Sören T-B, Lennartz B. Adsorption behaviour of Cr(VI) onto macro and micro-vesicular volcanic rocks from water. *Sep Purif Technol*. 2011;78:55-61. doi:10.1016/j.seppur.2011.01.020.
31. Asere TG, Mincke S, De Clercq J, et al. Removal of arsenic (V) from aqueous solutions using chitosan–red scoria and chitosan–pumice blends. *Int J Environ Res Public Health*. 2017;14:895. doi:10.3390/ijerph14080895.
32. Lemougna PN, Wang K-t, Tang Q, et al. Review on the use of volcanic ashes for engineering applications. *Resour Conserv Recycl*. 2018;137:177-190. doi:10.1016/j.resconrec.2018.05.031.
33. Federal Democratic Republic of Ethiopia, Ministry of Mines. *Strategic Assessment of the Ethiopian Mineral Sector Final Report*. Addis Ababa, Ethiopia: Federal Democratic Republic of Ethiopia, Ministry of Mines; 2014. https://openknowledge.worldbank.org/bitstream/handle/10986/20585/891390REVISED00260201400FOR0WEBF002.pdf?sequence=1&isAllowed=y.
34. Makita Y, Sonoda A, Sugiura Y, et al. Preparation and phosphate adsorptive properties of metal oxide-loaded granular activated carbon and pumice stone. *Colloids Surfaces A Physicochem Eng Asp*. 2019;582:123881. doi:10.1016/j.colsurfa.2019.123881.
35. Onar AN, Balkaya N, Akyüz T. Phosphate removal by adsorption. *Environ Technol*. 1996;17:207-213. doi:10.1080/09593331708616378.
36. Onar AN, Öztürk B. Adsorption of phosphate onto pumice powder. *Environ Technol*. 1993;14:1081-1087. doi:10.1080/09593339309385385.
37. Kim JY, Balathanigaimani MS, Moon H. Adsorptive removal of nitrate and phosphate using MCM-48, SBA-15, chitosan, and volcanic pumice. *Water Air Soil Pollut*. 2015;226:431. doi:10.1007/s11270-015-2692-z.
38. Liu C, Evett J. *Soil Properties: Testing, Measurement, and Evaluation*. 6th ed. Upper Saddle River, NJ: Pearson; 2008.
39. Sepehr MN, Zarrabi M, Kazemian H, Amrane A, Yaghmaian K, Ghaffari HR. Removal of hardness agents, calcium and magnesium, by natural and alkaline modified pumice stones in single and binary systems. *Appl Surf Sci*. 2013;274:295-305. doi:10.1016/j.apsusc.2013.03.042.
40. Ismail AIM, El-Shafey OI, Amr MHA, El-Maghraby MS. Pumice characteristics and their utilization on the synthesis of mesoporous minerals and on the removal of heavy metals. *Int Sch Res Notices*. 2014;2014:259379. doi:10.1155/2014/259379.
41. ALmilly RF, Hasan MH. Waste water treatment by liquid-solid adsorption using calcined sand-clay mixture adsorbent. *Iraq J Chem Pet Eng*. 2017;18:69-81.
42. American Public Health Association. *Standard Methods for the Examination of Water and Wastewater*. 21st ed. Washington, DC: American Public Health Association, American Water Works Association, Water Environment Federation; 2005.

43. Barrow NJ, Shaw TC. Effects of ionic strength and nature of the cation on desorption of phosphate from soil. *Eur J Soil Sci*. 1979;30:53-65. doi:10.1111/j.1365-2389.1979.tb00964.x.
44. Ali I, Gupta VK. Advances in water treatment by adsorption technology. *Nat Protoc*. 2006;1:2661-2667.
45. Nethaji S, Sivasamy A, Mandal AB. Adsorption isotherms, kinetics and mechanism for the adsorption of cationic and anionic dyes onto carbonaceous particles prepared from Juglans regia shell biomass. *Int J Environ Sci Technol*. 2013;10:231-242. doi:10.1007/s13762-012-0112-0.
46. Foo KY, Hameed BH. Insights into the modeling of adsorption isotherm systems. *Chem Eng J*. 2010;156:2-10. doi:10.1016/j.cej.2009.09.013.
47. Yavuz M, Gode F, Pehlivan E, Ozmert S, Sharma YC. An economic removal of Cu^{2+} and Cr^{3+} on the new adsorbents: pumice and polyacrylonitrile/pumice composite. *Chem Eng J*. 2008;137:453-461. doi:10.1016/j.cej.2007.04.030.
48. Kyzas GZ, Kostoglou M. Green adsorbents for wastewaters: a critical review. *Materials (Basel)*. 2014;7:333-364. doi:10.3390/ma7010333.
49. Ho YS, McKay G. A comparison of chemisorption kinetic models applied to pollutant removal on various sorbents. *Process Saf Environ Prot*. 1998;76:332-340. doi:10.1205/095758298529696.
50. Weber WJ, Morris JC. Kinetics of adsorption on carbon from solution. *J Sanit Eng Div*. 1963;89:31-60.
51. Ayawei N, Ebelegi AN, Wankasi D. Modelling and interpretation of adsorption isotherms. *J Chem*. 2017;2017:3039817. doi:10.1155/2017/3039817.
52. Kundu S, Gupta AK. Arsenic adsorption onto iron oxide-coated cement (IOCC): regression analysis of equilibrium data with several isotherm models and their optimization. *Chem Eng J*. 2006;122:93-106.
53. Langmuir I. The constitution and fundamental properties of solids and liquids. *J Am Chem Soc*. 1916;38:2221-2295.
54. Chaker M. Applicability of some statistical tools to predict optimum adsorption isotherm after linear and non-linear regression analysis. *J Hazard Mater*. 2008;153:207-212. doi:10.1016/j.jhazmat.2007.08.038.
55. Aregu MB, Asfaw SL, Khan MM. Identification of two low-cost and locally available filter media (pumice and scoria) for removal of hazardous pollutants from tannery wastewater. *Environ Syst Res*. 2018;7:10. doi:10.1186/s40068-018-0112-2.
56. Sperlich A, Werner A, Genz A, Amy G, Worch E, Jekel M. Breakthrough behavior of granular ferric hydroxide (GFH) fixed-bed adsorption filters: modeling and experimental approaches. *Water Res*. 2005;39:1190-1198. doi:10.1016/J.WATRES.2004.12.032.
57. Burgot JL. *Ionic Equilibria in Analytical Chemistry*. New York, NY: Springer; 2012. doi:10.1007/978-1-4419-8382-4.
58. Asgari G, Roshani B, Ghanizadeh G. The investigation of kinetic and isotherm of fluoride adsorption onto functionalize pumice stone. *J Hazard Mater*. 2012;217-218:123-132. doi:10.1016/j.jhazmat.2012.03.003.
59. Gormley-Gallagher AM, Douglas RW, Rippey B. The applicability of the distribution coefficient, K_D, based on non-aggregated particulate samples from lakes with low suspended solids concentrations. *PLoS ONE*. 2015;10:e0133069. doi:10.1371/journal.pone.0133069.
60. Rahdar S, Taghavi M, Khaksefidi R, Ahmadi S. Adsorption of arsenic (V) from aqueous solution using modified saxaul ash: isotherm and thermodynamic study. *Appl Water Sci*. 2019;9:87. doi:10.1007/s13201-019-0974-0.
61. Lee SY, Choi JW, Song KG, Choi K, Lee YJ, Jung KW. Adsorption and mechanistic study for phosphate removal by rice husk-derived biochar functionalized with Mg/Al-calcined layered double hydroxides via co-pyrolysis. *Compos Part B Eng*. 2019;176:107209. doi:10.1016/j.compositesb.2019.107209.
62. Robati D. Pseudo-second-order kinetic equations for modeling adsorption systems for removal of lead ions using multi-walled carbon nanotube. *J Nanostruct Chem*. 2013;3:55.
63. Riahi K, Chaabane S, Thayer BB. A kinetic modeling study of phosphate adsorption onto Phoenix dactylifera L. date palm fibers in batch mode. *J Saudi Chem Soc*. 2017;21:S143-S152. doi:10.1016/j.jscs.2013.11.007.
64. Chen J, Cai Y, Clark M, Yu Y. Equilibrium and kinetic studies of phosphate removal from solution onto a hydrothermally modified oyster shell material. *PLoS ONE*. 2013;8:e60243. doi:10.1371/journal.pone.0060243.
65. Ethiopian Environmental Protection Authority. *Provisional Standards for Industries*. Addis Ababa, Ethiopia: Ethiopian Environmental Protection Authority; 2008:1-24.
66. Momina Rafatullah M, Ismail S, Ahmad A. Optimization study for the desorption of methylene blue dye from clay based adsorbent coating. *Water (Switzerland)*. 2019;11:1304. doi:10.3390/w11061304.
67. Loebenstein WV. Adsorption, desorption, resorption. *J Res Natl Bur Stand A Phys Chem*. 1963;67A:615-624. doi:10.6028/jres.067a.061.